**Structural Engineering and Mechanics**, *Vol. 62, No. 1 (2017) 79-84*
DOI: https://doi.org/10.12989/sem.2017.62.1.079 

# Numerical modeling of semi-confined composite beams consisting of GFRP and concrete

Amir Masoud Hassanzadeh[a] and Mehdi Dehestani*

*Faculty of Civil Engineering, Babol Noshirvani University of Technology, Babol, Iran*

*(Received October 10, 2015, Revised January 3, 2017, Accepted January 23, 2017)*

**Abstract.** Utilizing composite members in structures has been considered by many researchers in the past few decades. Using FRP can be very effective owing to its excessively high-tensile strength, which compensate concrete weak performance in tension. In this research, the studied composite beam includes a GFRP semi-confined trapezoidal section covered by GFRP and concrete layers. To assess the bearing capacity, a finite-element model of a composite beam subjected to displacement control loading has been developed and the results were validated using experimental results found throughout the literature. Several parameters affecting the bending performance and behavior of the semi-confined beam have been investigated in this study. Some of these parameters included the thickness of GFRP trapezoidal section members, concrete layer thickness, GFRP layer thickness and the confinement degree of the beam. The results revealed that the beam confinement had the highest effect on the bearing capacity due to prevention of separation of concrete from GFRP which causes the failure of the beam. From the results obtained, an optimal model of primary beam section has been introduced, which provides a higher bearing capacity with the same volume of materials used in the original beam section.

**Keywords:** concrete; GFR; composite beam; finite-element; confinement

## 1. Introduction

Accelerated construction and cost effective methods along with decreased structural weight have always been important goals for civil engineers and researchers. Using FRP with classic materials such as concrete and steel would help to achieve these goals. Over the past few years, the use of FRP has become very popular among researchers because of its natural properties such as low weight (with a density of about 0.2 of steel), high-tensile strength, high resistance to corrosion, magnetic impermeability, capability of external strengthening, easy transportation and high implementation speed. Advanced polymer composites are important for a variety of industrial applications, including building industry, bridge enclosures and fairing, bridge decks, external reinforcement rehabilitation, retrofitting of RC structures (including FRP confined concrete columns), polymer bridge bearings, vibration absorbers, retrofitting of steel structures and regarding demerits of GFRP. FRPs are yet to become a mainstream application due to a number of economical and design related issues. It is notable that limited experience with FRP materials in the construction industry, lack of performance history, sensibility to static fatigue under tensile loading, the potential of brittle debonding failures, the need for different saw blades and drill are known as drawbacks in this area.

Various properties have resulted in different uses of FRP, for example, the use of FRP bars instead of metal bars to increase damping of vibrations caused by the earthquake was suggested by Bank (2007), Kim and Yoon DK (2010). The production of pre-built FRP profiles and its use in beams and decks in bridge construction which is more exposed to environmental damages according toits lower weight and higher corrosion strength was investigated by Bakis *et al*. (2002).

A special type of FRP, which has gained attention over the past few years, is Glass-FRP (GFRP) that is more commonly used due to its lower price compared to its other derivatives like AFRP or CFRP. GFRPs are divided into various types based on the composition of materials in its preparation. Fardis and Khalili (1981) were the first researchers who introduced the idea of designing a GFRP confined beam with rectangular section. The beams with FRP casing had very good strength and ductility. Mouri and Hillman (1990) used the combination of prefabricated FRP sections and concrete to build beam and slab. The use of FRP led to a significant decrease in structure weight. Saidi (1994) offered a beam model in which a concrete reinforced deck had been placed on a CFRP beam. He used shear connecter and epoxy glue to connect the concrete reinforced deck to prefabricated CFRP section.

Keller *et al*. (2006) promoted a hybrid sandwich deck model, including concrete and FRP in which the concrete core had been confined in GFRP tensile panel and a GFRP pressure plate. Mechanical tests on eight hybrid beams were conducted with two types of interface: unbonded (only mechanical interlocking) and bonded with an epoxy adhesive. The ultimate strengths of beams increased about 104% due to improved bonding. However, the failure mode of beam has been changed from ductile to brittle. Lee

*Corresponding author, Associate Professor
E-mail: dehestani@nit.ac.ir
[a]Graduate Student


http://www.techno-press.org/?journal=sem&subpage=8 ISSN: 1225-4568 (Print), 1598-6217 (Online)

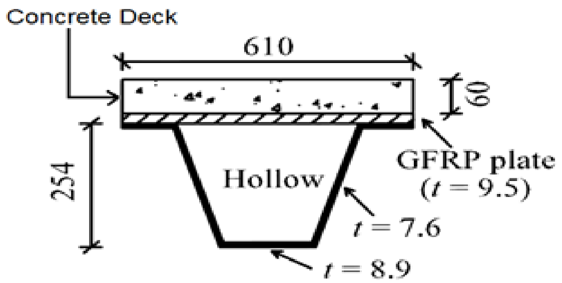


Fig. 1 $M_1$ section

(2006) tested a composite beam consisting of a GFRP I-shaped profile covered by a concrete slab. He built several concrete specimens with different compressive strengths and thicknesses; and the system failure was occurred with the formation of horizontal shear cracks in GFRP beam. In the specimens with higher slab thickness, tensile cracking has been observed in the concrete.

Aydin and Sarik (2011) tested a rectangular section of GFRP. They conducted several experiments on four types of specimens. The specimens include a GFRP rectangular section; a concrete filled GFRP section; a sand-covered GFRP section filled with concrete; and fiber- wrapped GFRP section filled with sand. The highest bending capacity was observed in this last case.

Jeng (2007) offered a new section for beam and column, Hybrid FRP-concrete-steel double-skin tubular columns which included an internal metal tube, an external FRP tube layer and concrete to fill the gap between two layers, and the internal space would be filled or left empty. A series of axial compression tests were performed on stub columns. The experimental results illustrated that the GFRP tube increases the structure bearing capacity by confining the concrete.

De Sutter *et al*. (2014) performed an experimental study on composite beams containing a U-shape section and hollow core elements. They used ultra-high performance concrete and CFRP at the outer and inner side of hollow element, respectively. It is shown that a composite beam with the same stiffness has a greater bearing capacity and lower weight in comparison with traditional reinforced concrete beams. Idris *et al*. (2014) examined flexural performance of hybrid beams. In their prototype beam, the tube was composed of inner and outer layers made of steel and FRP, respectively. The space between them was filled with concrete. It was reported that the diameter and thickness of the inner steel tube significantly influenced the flexural behavior of the beam. In addition, enhanced concrete strength increases the flexural capacity of the beam as well.

Alizadeh and Dehestani (2015) studied the efficiency of GFRP box girders by changing GFRP material to steel and aluminum and examined the effects of component's properties by changing the compressive strength of concrete slab and Elastic modulus of GFRP materials. Moreover, the effect of cross-sectional configuration was assessed. It was concluded that the ultimate load capacity is enhanced by deformation of composite girder cross-section, and the strength-to-weight ratio of the girder is increased by changing the GFRP material to aluminum.

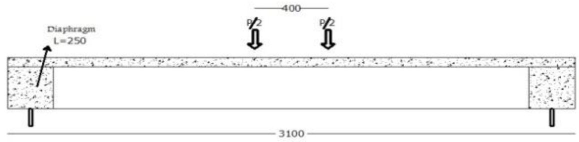


Fig. 2 Loading method for the original $M_1$ model in laboratory

### 1.1 Research significance

Kim and Fam (2011) studied parameters affecting composite beam bearing capacity with the use of a finite-element model. They studied composite beams with concrete and FRP, and proposed several models in this field. The accuracy of the finite-element model was validated by laboratory tests results. This study, evaluated the effect of some parameters such as GFRP trapezoidal section dimensions thickness, GFRP layer thickness, concrete layer thickness and confinement on the bearing capacity of structure, and finally; an optimal model is designed for beam section. The degree of confinement has been one of the important and useful tools in performance of composite beams subjected to displacement control loading in this field and has been rarely received any attention in previous research. The investigation and comparison of the above parameters can provide a proper view for optimal designing of composite beam section.

## 2. Composite beam and finite element modeling

As shown in Fig. 1, the composite beam, called $M_1$, includes a GFRP trapezoidal section with a height of 254 mm, width of 610 mm and length of 3350 mm. A flat GFRP layer of 9.5 mm thickness is stuck over the GFRP trapezoidal section through high shear strength glue. A 60 mm concrete layer covers the GFRP flat layer. Inside the concrete, a row of (76 mm×76 mm×3 mm) bars is embedded to control the crack propagation caused by concrete shrinkage. Furthermore, since the inside of the trapezoidal section is hollow, a concrete component with a length of 250mm is placed on two supports to prevent beam cracking by enabling extra shear strength on the beam edges. Loading regime on the studied beam is according to Fig. 2. The loading type is displacement control at a rate of 1 mm/min with a certain distance from the beam center with 400mm gaps between them. Rigid plates are also considered infinite element elements to prevent the concentration of stress on the concrete surface subjected to direct load, so the load would be put on these plates. The support conditions are also considered simple, and in fact, two components with excessive stiffness are considered as the support which are considered to be tied with no degrees of freedom.

Abaqus 6.14 software has been used for finite-element modelling. The trapezoidal section and the plate stuck on it are GFRP type and modelled as four-node shell hexahedron element. The behavioural characteristics of GFRP are

Table 1 Material properties of GFRP composites from (Fam and Honickman 2010)

| | | GFRP trapezoidal section | | GFRP plate | |
|---|---|---|---|---|---|
| | | Longitudinal | transverse | Longitudinal | Transverse |
| Elastic Module (GPa) | tension | 26.2 | 11.2 | 6.9 | 12.4 |
| | pressure | 26.2 | 11.2 | 6.9 | 12.4 |
| Strength (MPa) | tension | 517 | 138 | 68.7 | 137.5 |
| | pressure | 345 | 172 | 110 | 165 |

modelled orthotropic and presented in Table 1. As mentioned, two GFRP types are used for the plate and trapezoidal section in this composite beam, and they have different tensile and compressive strengths. The strain-stress changes in GFRP are considered as being elastic, and it is assumed with natural FRP characteristics. To model concrete reinforced layer, solid element has been used, which is capable of demonstrating cracking and crushing and this means that when the main stress in elements exceeds the allowable stress, the cracking occurs. Initially, the concrete properties are considered isotropic, and as soon as a crack is created, its properties will be changed to orthotropic. Mesh density is considered in a way that the maximum size of each mesh would be 50 mm. the interaction between elements is modelled as Tie. Two different methods are used to model the adhesive bond between the concrete layer and the FRP. In the first method, cohesive elements are used, which requires the mechanical properties of the adhesive including the stiffness values for *Knn/Kss/Ktt*, which can be estimated based upon the modulus of the bonding material but typically some types of experimental correlation are required to determine the exact value to use. These values are taken from coupon testing of the bonding material such as a peel test for the normal stiffness and a lap joint test for the shear dominated stiffness Tie interaction is used in the other method, by which the user is basically enabled to join two surfaces of different meshing schemes, and This simulates a perfect bond and does not allow the two surfaces to translate relative to each other. In this study, the Tie interaction was used, since the required stiffness parameters were not included in the mentioned experimental study to model the adhesive bond.

This simulates a perfect bond and does not allow the two surfaces to translate relative to each other. Therefore, the contact surface between concrete and GFRP plate is considered to have no slippage. To measure the force applied to the composite beam, after several investigations performed in different areas of the beam, the area below the rigid plates was identified as displacement control to measure the bearing capacity of the structure subjected to loading.  The load was monotonically applied at a loading rate of 1 mm/min (Fig. 2). The strain gauges were installed at the mid-span of the girder, on the top of concrete slab and bottom of the hat-shape section.

Existed data in the literature, by Kim and Fam (2011) have been used to validate the behaviour of the presented model. The geometric properties of the studied beam are shown in Fig. 1. To validate the modelling, the results of loading with displacement control in the laboratory were compared with results of the finite-element model. As observed, the force per displacement chart moves linearly up to 278 kN, and then it breaks down. In the laboratory model, the composite beam reaches a displacement of 28mm by applying a force of 285 kN and yields. Therefore, in the finite-element model, the load is applied as displacement control with a value of 28 mm, as shown in Fig. 2, and its bearing capacity reaches the final force of 278 kN. In Fig. 3, a comparison between the force charts based on composite beam displacement has been demonstrated in both laboratory and finite-element states. This comparison shows that there is a good consistency between laboratory and finite-element models in terms of final load value and plasticity. Furthermore, the concrete separation from GFRP layer by applying displacement to beam can be observed in Fig. 4. Fig. 5 shows the stress contour of the composite beam in the perspective of a cut from the middle, and thus the stress at the internal levels of GFRP trapezoidal section. The properties of all models are given in Table 2. The mentioned table was adopted from Fam and Honickman (2010) paper. In fact, the GFRP properties are prepared in the factory according to the requirements demanded by the order.

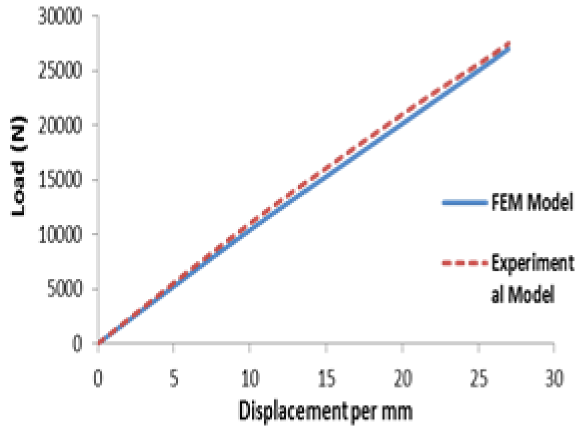


Fig. 3 Comparison between charts of force per displacement of finite element model and Experimental model

## 3. Parametric analysis

The GFRP trapezoidal section thickness is the first parameter studied, and the effects of these modifications on the main composite beam bearing capacity, called $M_1$, has been investigated. With changing a parameter by a certain value, the other parameters were kept constant. All of parameters are shown in Fig. 6, where the thickness of concrete layer is shown by $T_c$, GFRP layer thickness by $T_G$, the thickness of GFRP trapezoid section's upper base by $T_u$, the GFRP trapezoidal web thickness by $T_d$, the thickness of lower base of GFRP by $T_b$, and the length of confinement by Le. In the first scenario, $M_1$ is examined as the original sample of the main beam in the laboratory (Fig. 1). In the second scenario, $M_2$, the web thickness $T_d$ was increased

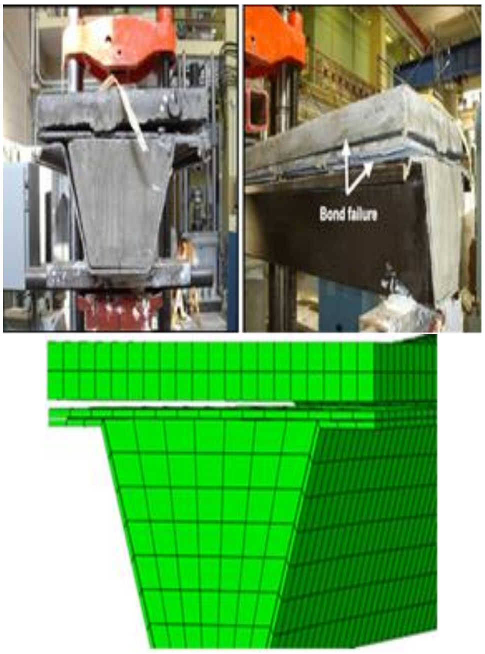


Fig. 4 Debonding between concrete and GFRP layer in laboratory and finite element model

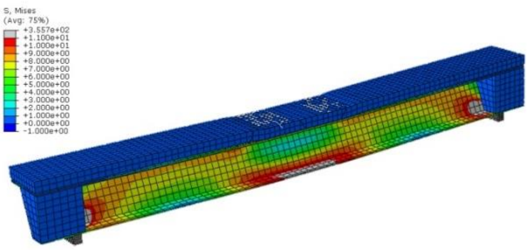

Fig. 5 Von Mises stress contour in the main beam $M_1$

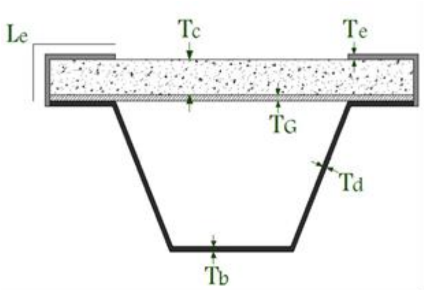


Fig. 6 Sectional parameters

25% and reached 9.5 mm from initial 7.6 mm by maintaining the thickness of upper base $T_u$ and lower base $T_b$ of trapezoidal section constant. In consequence, its bearing capacity reaches 315 kN from previous 278 kN. Since the lengths of trapezoidal section sides are different, then in any situation, the added thickness is to an extent that the total weight and area are equal in all three scenarios. In the third scenario, $M_3$, by maintaining the web and upper base thicknesses constant, the thickness of lower base was increased with a value, so the added level and weight would be equal to $M_2$ state. Its capacity increased from 278 kN to 311 kN. In the fourth scenario, which is called $M_4$, the

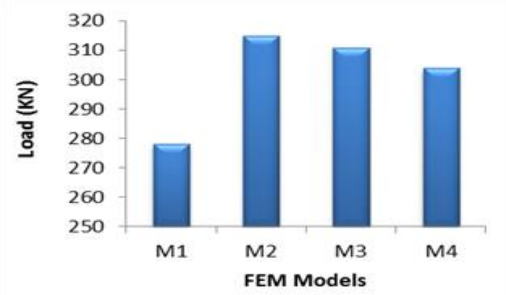


Fig. 7 Beam bearing capacity per different thicknesses of section

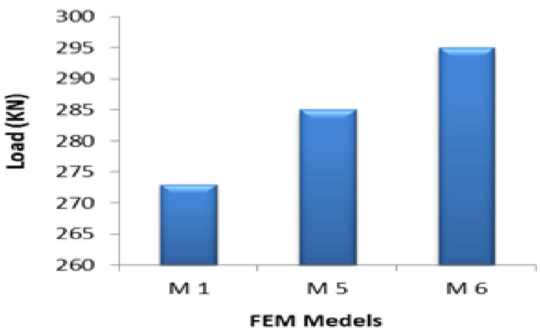


Fig. 8 Bearing capacity with different thickness of GFRP layer and concrete

thickness of upper base is increased from 8.9 mm to 14.04 mm, by maintaining the web thickness and the lower base constant.

As a result, the bearing capacity is increased from 278 kN to 305 kN. By comparing the above states, it can be discovered that the web thickness has the highest effect on bearing capacity compared to other parts of trapezoidal section. The outcome states the shear performance of beam is more important than its bending performance in this state. The results are available in Fig. 7.

In this study, the GFRP layer’s thickness and the concrete deck of $M_1$ model have been changed, and the results are shown in Fig. 8. In $M_5$ scenario, the GFRP flat layer thickness was increased, and the beam bearing capacity was increased from 278 kN to 285 kN. In another scenario, $M_6$, only the concrete thickness was increased, while the GFRP layer thickness was remained constant. As a result of this change, the bearing capacity was increased from 278 kN to 295 kN.

## 4. Investigating the effects of confinement

The original model with different length and thickness of confinement is analysed in order to demonstrate the effects of confinement on beam behaviour. The elimination of the need for form working which results in simplicity of implementation and economic saving are considered some advantages of confinement. Fig. 6 shows the way the section is confined with Le parameter. In $M_7$ scenario as shown in Fig. 10, the confinement with a length of 78.4 mm and thickness of 8.9 mm extends to the edge of concrete and

Table 2 Properties of models

| Finite element models | Upper base thickness $T_u$ (mm) | Lower base thickness $T_b$ (mm) | Web thickness $T_d$ (mm) | GFRP layer thickness $T_G$ (mm) | Concrete layer thickness $T_c$ (mm) | Confinement degree $L_e$ (mm) | Confinement thickness $T_e$(mm) | Bearing capacity (KN) |
|---|---|---|---|---|---|---|---|---|
| $M_1$ | 8.9 | 8.9 | 7.6 | 9.5 | 60 | 0 | 0 | 278 |
| $M_2$ | 8.9 | 8.9 | 9.5 | 9.5 | 60 | 0 | 0 | 315 |
| $M_3$ | 8.9 | 13.5 | 7.6 | 9.5 | 60 | 0 | 0 | 311 |
| $M_4$ | 14.0 | 8.9 | 7.6 | 9.5 | 60 | 0 | 0 | 304 |
| $M_5$ | 8.9 | 8.9 | 7.6 | 11.9 | 75 | 0 | 0 | 285 |
| $M_6$ | 8.9 | 8.9 | 7.6 | 9.5 | 60 | 0 | 0 | 295 |
| $M_7$ | 8.9 | 8.9 | 7.6 | 9.5 | 60 | 69.5 | 8.9 | 359 |
| $M_8$ | 8.9 | 8.9 | 7.6 | 9.5 | 60 | 117.3 | 4.8 | 391 |
| $M_9$ | 8.9 | 8.9 | 7.6 | 9.5 | 60 | 174.1 | 3.7 | 402 |

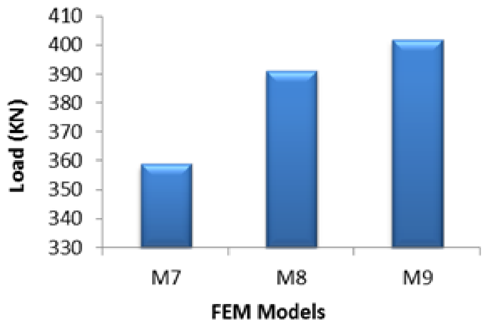


Fig. 9 Chart of beam bearing capacity per confinement

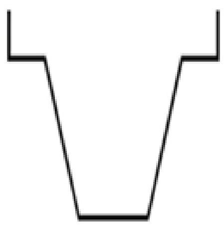

Fig. 10 $M_7$ model

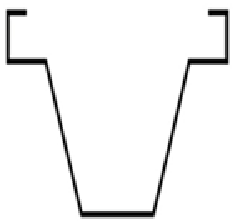

Fig. 11 $M_8$ model

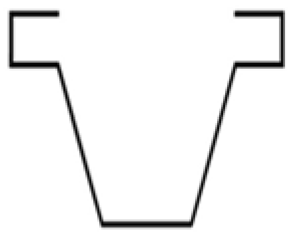

Fig. 12 $M_9$ model

the new model is analysed and the value of final load is increased from 278 kN to 359 kN In state $M_{8,}$ in which the section is shown in Fig. 11, the degree of confinement with length of 144 mm is extended to the middle of upper trapezoid base; and for the confined level degree added to the beam to be equal in all the examination states, the thickness of confined level is decreased from 8.9 mm to 4.8 mm, so the value of final load is increased from 278 kN to 391 kN. In $M_9$ scenario, which can be observed in Fig. 12, the confinement with a length of 200.75 mm extends to the trapezoidal section upper base, and due to the equality of the confined level, its thickness reaches 3.47 mm; and the final load bearing is increased from 278 kN to 402 kN. As shown, the confinement parameter is introduced as the most effective parameter because it prevents separation between concrete and GFRP layer.

## 5. Presenting an optimal design of composite beam

Finite-element method was used to investigate bearing capacity of the composite beam, and the results were verified using previous works found in the literature. This research studied the effects of the a number of parameters such as the thickness of trapezoidal section, GFRP layer thickness, concrete layer thickness, and beam degree of confinement on composite beam bearing capacity; and the results of this investigation are presented above. The goal was to achieve higher bearing capacity with the same amount of materials. As investigated, beam confinement has the highest effects on the load-bearing capacity; and also, by modifying the thickness of various parts of the trapezoidal beam, it is found that the web thickness has the highest effect on the beam performance.

Therefore, it is tried to decrease the upper and the lower base thickness of trapezoidal section, and increase the beam confinement in the same degree by maintaining the web thickness.

At this stage, the purpose of composite beam optimization is to achieve higher bearing capacity with the same amount of primary materials. According to evaluation, because beam confinement prevents separation between the concrete and GFRP layer, it has the highest effect on final load bearing capacity of the beam; and the web thickness has the greatest effect among the trapezoidal thickness of section.

Therefore, it is tried to reduce the thickness of the upper and the lower base of the trapezoidal section, and increasing the beam confinement with the same amount. As evaluated, the highest bearing capacity was observed where confinement extends to lower base, but since this can be difficult for implementing and placing the GFRP layer and sticking it to the trapezoidal section, the confinement state is considered to be extended upward to the middle of base.

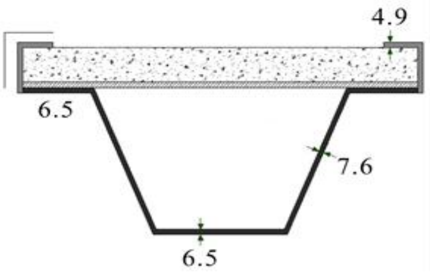

Fig. 13 Section of optimal beam

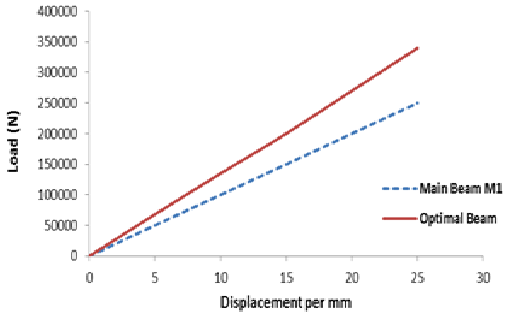

Fig. 14 Comparison between force charts based on the displacement of primary beam and optimized beam

In this state, According to Fig. 13, the web thickness is not changed and has the same value of 7.6 mm. The thickness of upper and lower bases is decreased from 8.9 mm to 6.5 mm, and the beam confinement with a thickness of 4.9 mm is extended to the middle of base. As a result of these changes, the bearing capacity of the optimal composite beam is increased from 278 kN to 357 kN. Fig. 14 shows a comparison between optimized composite beam and its primary state.

## 6. Conclusions

In this research, the studied composite beam included a GFRP trapezoidal section on which a flat GFRP layer was glued. A concrete layer placed over the GFRP flat layer. Loading on the beam was implied with a displacement control. Initially, this research investigated the several parameters influencing the semi-confined composite beam bending performance and behavior. These parameters included changing thicknesses of upper base of GFRP trapezoidal section, web and lower base, concrete layer, GFRP flat layer, and the confinement degree on the beam bearing capacity. By contrasting the thickness parameters, it was concluded that the trapezoidal web thickness of section had the highest effect on the bearing capacity of the beam compared to the thickness of other parts of trapezoidal section, and thus the shear performance of the beam in this state is more important than its bending performance, so the effect of changing the web thickness was more important than the wing. Since the beam confinement prevents separation of the concrete and GFRP layer and consequently, the beam failure; it is introduced as the most important parameter on the composite bearing capacity of the beam. In $M_2$ to $M_7$ samples shear failures occurred due to the separation of the concrete and GFRP layer, but in $M_8$ and $M_9$ models, the structure failure occurred due to mid-beam crushing, which is bending failure. Finally, an optimal section is presented for the composite beam by evaluating studied parameters, so a higher bearing capacity is obtained with the same volume of materials used in primary section of the beam.

## References

Alizadeh, E. and Dehestani, M. (2015), "Analysis of composite girders with hybrid GFRP hat-shape sections and concrete slab", *Struct. Eng. Mech.*, **54**(6), 1135-1152.

Aydın, F. and Sarıbıyık, M. (2013), "Investigation of flexural behaviors of hybrid beams formed with GFRP box section and concrete", *Constr. Build. Mater.*, **41**, 563-569.

Bakis, C., Bank, L. C., Brown, V., Cosenza, E., Davalos, J. F., Lesko, J. J., ... and Triantafillou, T. C. (2002), "Fiber-reinforced polymer composites for construction-state-of-the-art review", *J. Compos. Construct.*, **6**(2), 73-87.

De Sutter, S., Remy, O., Tysmans, T. and Wastiels, J. (2014), "Development and experimental validation of a lightweight stay-in-place composite formwork for concrete beams", *Constr. Build. Mater.*, **63**, 33-39.

Deskovic, N., Triantafillou, T. C. and Meier, U. (1995), "Innovative design of FRP combined with concrete: short-term behavior", *J. Struct. Eng.*, **121**(7), 1069-1078.

Fam, A. and Honickman, H. (2010), "Built-up hybrid composite box girders fabricated and tested in flexure", *Eng. Struct.*, **32**(4), 1028-1037.

Fam, A., Schnerch, D. and Rizkalla, S. (2005), "Rectangular filament-wound glass fiber reinforced polymer tubes filled with concrete under flexural and axial loading: experimental investigation", *J. Compos. Construct.*, **9**(1), 25-33.

Fardis, M.N. and Khalili, H. (1981), "Concrete encased in fiberglass-reinforced plastic", *J. Am. Concrete Inst.*, **78**(6), 440-446.

Hibbitt, D., Karlsson, B. and Sorensen, P. (2004), ABAQUS Analysis User's Manual, Pawtucket, USA.

Ji, H.S., Byun, J.K., Lee, C.S., Son, B.J. and Ma, Z.J. (2011), "Structural performance of composite sandwich bridge decks with hybrid GFRP-steel core", *Compos. Struct.*, **93**(2), 430-442.

Keller, T., Schaumann, E. and Vallee, T. (2006), "Hybrid FRP-concrete sandwich bridge deck", *Proceedings of the 3rd International Conference on FRP Composites in Civil Engineering (CICE 2006)*, Miami, USA.

Kim, H.Y., Hwang, Y.K., Park, K.T., Lee, Y.H. and Kim, S.M. (2005), "Fiber reinforced plastic deck profile for I-girder bridges", *Compos. Struct.*, **67**(4), 411-416.

Kim, Y.J. and Fam, A. (2011), "Numerical analysis of pultruded GFRP box girders supporting adhesively-bonded concrete deck in flexure", *Eng. Struct.*, **33**(12), 3527-3536.

Kim, Y.J. and Yoon, D.K. (2009), "Identifying critical sources of bridge deterioration in cold regions through the constructed bridges in North Dakota", *J. Bridge Eng.*, **15**(5), 542-552.

Kitane, Y., Aref, A.J. and Lee, G.C. (2004), "Static and fatigue testing of hybrid fiber-reinforced polymer-concrete bridge superstructure", *J. Compos. Construct.*, **8**(2), 182-190.

Teng, J.G., Yu, T., Wong, Y.L. and Dong, S.L. (2007), "Hybrid FRP-concrete-steel tubular columns: concept and behavior", *Constr. Build. Mater.*, **21**(4), 846-854.

*CC*